Temperature: The "Ignored" Factor at the NanoBio Interface

Morteza Mahmoudi,[†,*] Abuelmagd M. Abdelmonem,[‡,¶] Shahed Behzadi,[†] Joachim H. Clement,[§] Silvio Dutz,[⊥] Mohammad R. Ejtehadi,[∥] Raimo Hartmann,[‡] Karsten Kantner,[‡] Uwe Linne,[‡] Pauline Maffre,[#] Scott Metzler,[△] Mojhgan K. Moghadam,[⊗] Christian Pfeiffer,[‡] Meisam Rezaei,[∥] Pilar Ruiz-Lozano,[△] Vahid Serpooshan,[△] Mohammad A. Shokrgozar,[⊗] G. Ulrich Nienhaus,[∞,#,*] and Wolfgang J. Parak[‡,▽,*]

[†]Nanotechnology Research Center and Department of Nanotechnology, Faculty of Pharmacy, Tehran University of Medical Sciences, Tehran, Iran, [‡]Fachbereich Physik/Chemie, Philipps-Universität Marburg, Marburg, Germany, [§]Department of Hematology/Oncology, University Hospital Jena, Friedrich-Schiller University Jena, Jena, Germany, [⊥]Department Nano Biophotonics, Institute of Photonic Technology, Jena, Germany, [∥]Department of Physics, Sharif University of Technology, Tehran, Iran, [∞]Department of Physics, University of Illinois at Urbana-Champaign, Urbana, Illinois, United States, [#]Institute of Applied Physics and Center for Functional Nanostructures (CFN) and Institute of Toxicology and Genetics (ITG), Karlsruhe Institute of Technology (KIT), Karlsruhe, Germany, [△]Department of Pediatrics, Division of Cardiology, School of Medicine, Stanford University, Stanford, California, United States, [⊗]National Cell Bank, Pasteur Institute of Iran, Tehran, Iran, and [▽]CIC Biomagune, San Sebastian, Spain. [¶]Contributing authors in alphabetic order.

ABSTRACT Upon incorporation of nanoparticles (NPs) into the body, they are exposed to biological fluids, and their interaction with the dissolved biomolecules leads to the formation of the so-called protein corona on the surface of the NPs. The composition of the corona plays a crucial role in the biological fate of the NPs. While the effects of various physicochemical parameters on the composition of the corona have been explored in depth, the role of temperature upon its formation has received much less attention. In this work, we have probed the effect of temperature on the protein composition on the surface of a set of NPs with various surface chemistries and electric charges. Our results indicate that the degree of protein coverage and the composition of the adsorbed proteins on the NPs' surface depend on the temperature at which the protein corona is formed. Also, the uptake of NPs is affected by the temperature. Temperature is, thus, an important parameter that needs to be carefully controlled in quantitative studies of bionano interactions.

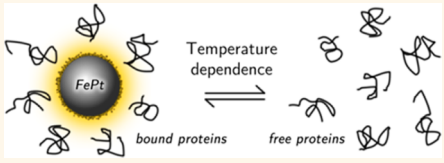

KEYWORDS: colloidal magnetic nanoparticles · protein corona · temperature dependence · uptake by cells · protein adsorption

Nanoparticles (NPs) are presently being employed in a wide variety of biomedical and biotechnological applications. In some applications, such as targeted drug delivery, researchers aim to develop NPs such that they are selectively incorporated by specific cell types in living tissue. In other applications, such as NP-based contrast agents for magnetic resonance imaging, NPs should stay in the bloodstream and subsequently be cleared by the kidneys, but not be internalized by cells. It is known that cellular NP uptake is strongly influenced by the NP size as well as their surface properties, including decoration by functional groups and biomolecules. A detailed understanding of the interactions between NPs and different cell types is key to understanding and controlling cellular uptake mechanisms.[1−4]

NPs entering the human body first come in contact with a biological fluid, *e.g.*, blood or lung-lining fluid. They interact with the dissolved biomacromolecules, in particular proteins, and an adsorption layer of proteins, the so-called "protein corona", forms around the NPs.[5−7] While protein adsorption onto planar surfaces has been investigated for decades, detailed studies of NP−protein interactions have only started recently.[8−13] Studies have especially focused on the effects of physicochemical parameters of NPs (*e.g.*, size, shape, composition, surface roughness, porosity, surface charge) on the formation of the protein corona.[14] The temperature, however, at which the NPs and the protein are maintained in solution likewise should be an important factor influencing the corona composition. For example, it has been shown that the composition of the protein corona formed upon NP exposure to heat-inactivated proteins (preheating at 56 °C) and non-heat-inactivated proteins is different.[15] As a result, significant differences were observed in the amounts of NPs taken up by cells. However, temperature effects close to physiological temperature (*i.e.*, not involving denaturation) on the

* Address correspondence to Mahmoudi-M@TUMS.ac.ir; uli@uiuc.edu; wolfgang.parak@physik.uni-marburg.de.

Received for review November 16, 2012 and accepted June 30, 2013.

Published online July 01, 2013
10.1021/nn305337c

protein corona have not yet been studied in detail. Those effects may be relevant for *in vivo* applications of NPs because body temperature can vary significantly. The mean human body temperature ranges from 35.8 to 37.2 °C and varies for different parts of the body.[16] It decreases during sleep and increases by up to 2 °C during physical activities and can even climb to 41 °C in the case of fever.[17] It is also known that the temperature in peripheral parts of the body (*e.g.*, skin) during exposure to cold weather can drop to 28 °C.[18] Very recently, even the intracellular temperature of living cells was shown to be inhomogeneous.[19,20]

If protein adsorption onto the surface of NPs depends on the body temperature, it may also result in a significant effect on the cellular uptake of NPs *in vivo*. Therefore, we have studied the influence of near-physiological temperature variation on the formation of the protein corona, using superparamagnetic NPs synthesized from different materials with different surface coatings and thus different ζ-potentials as model NPs. Magnetic NPs enable effective magnetic washing and separation, which is beneficial for handling of small amounts of NP sample. Precisely defined and well-characterized polymer-coated FePt NPs were incubated with human serum albumin (HSA) and apo-transferrin (apo-Tf) at different concentrations and temperatures, and the monolayer formation of adsorbed proteins was quantified by using fluorescence correlation spectroscopy (FCS). Moreover, larger FeO_x NPs (superparamagnetic iron oxide NPs, SPIONs) with positive and negative charge and also with neutral surfaces were incubated in fetal bovine serum (FBS) at different temperatures, and the compositions of the resulting coronae were analyzed as a function of the incubation temperature. We have also assessed the effect of the temperature-dependent corona composition on cellular uptake.

RESULTS AND DISCUSSION

Temperature Dependence of HSA and apo-Tf Monolayer Formation on FePt NPs. For our protein adsorption studies we used fluorescently labeled, negatively charged polymer-coated FePt NPs. The inorganic core diameter, d_c, was determined by transmission electron microscopy (TEM). The hydrodynamic diameter, d_h, was measured by dynamic light scattering (DLS, *cf.* Table 1) and fluorescence correlation spectroscopy (FCS, *cf.* Table 2) at room temperature in phosphate-buffered saline (PBS). Results obtained with the FCS method (d_h = 12.0 ± 0.2 nm and 10 ± 0.4 nm for two different batches at room temperature) are very precise and reproducible and have been verified in several independent studies.[21−24] The DLS data on bare NPs without proteins (d_h = 10 ± 5 nm) are—within experimental error—in agreement with the FCS data but have larger margins of error.[21,24] Furthermore, the FCS data (*cf.* Table 2) indicate that temperature variation between 9 and 43 °C does not affect the hydrodynamic diameter of the bare FePt NPs. Thus, the polymer surface of these NPs can be considered to be stable in this temperature range. In a previous study, we also demonstrated that the polymer shell of the NPs dissolved in PBS remains stable over time.[14]

TABLE 1. Core (d_c) and Hydrodynamic (d_h) Diameters of NPs As Determined with TEM and DLS (at room temperature in PBS)

NP material	charge	d_c [nm]	d_h [nm]
FePt	Negative	3.5 ± 0.6	10 ± 5
FeO_x	Negative	15 ± 5	33 ± 8
FeO_x	Neutral	22 ± 7	33 ± 10
FeO_x	Positive	17 ± 5	79 ± 7

TABLE 2. Temperature-Dependent Protein Adsorption onto FePt NPs As Derived from FCS Measurements in PBS[a]

	HSA				
T [°C]	$r_h(0)$ [nm]	$r_h(N_{max})$ [nm]	K'_D [μM]	n	N_{max}
13	5.5 ± 0.3	9.2 ± 0.4	10 ± 4	0.6 ± 0.1	31 ± 5
23	6.0 ± 0.1	9.3 ± 0.2	6.3 ± 2.2	0.9 ± 0.2	30 ± 3
43	6.0 ± 0.1	8.8 ± 0.2	0.8 ± 0.4	0.7 ± 0.2	23 ± 2
	Apo-Tf				
T [°C]	$r_h(0)$ [nm]	$r_h(N_{max})$ [nm]	K'_D [μM]	n	N_{max}
9	5.1 ± 0.2	15.1 ± 0.8	13 ± 4	0.6 ± 0.1	47 ± 7
22	5.0 ± 0.2	14.3 ± 0.7	16 ± 6	0.7 ± 0.1	40 ± 6
43	5.3 ± 0.1	11 ± 0.4	5 ± 1	0.7 ± 0.1	17 ± 2

[a] $r_h(0)$ and $r_h(N_{max})$ are the hydrodynamic radii of NPs without adsorbed proteins and upon saturation of the NP surface with proteins, respectively; n is the Hill coefficient, which controls the steepness of the binding curve, N_{max} is the maximum number of proteins adsorbing onto a single NP, and K'_D represents the concentration of protein molecules at half coverage. Data for two different proteins are shown, HSA and apo-Tf.

Protein adsorption was quantified in terms of changes in hydrodynamic radius, $r_h = d_h/2$, of the NPs by using FCS. We studied the adsorption of HSA and apo-Tf, two important serum proteins, onto polymer-coated FePt NPs. Please note that, due to the small size of the NPs and due to the thin protein shell (which provides only little contrast), TEM turned out not to be the method of choice for the analysis of the protein corona (*cf.* Supporting Information). FCS analysis was performed directly on NP solutions with varying protein concentrations. Because the fluorescent labels reside in the polymer shell of the FePt NPs and not on the proteins, there was no need for purification steps to remove unbound proteins, which may introduce errors in the quantitative assessment of protein−NP interactions. Thus, FCS measurements allow for the direct analysis of the proteins forming the protein corona *in situ*. Because the surface of our polymer-coated FePt NPs is homogeneous, a spherical shape will be maintained under saturating conditions, *i.e.*, when the whole NP surface is covered with protein. In the other limit, *i.e.*, upon binding of only one or two

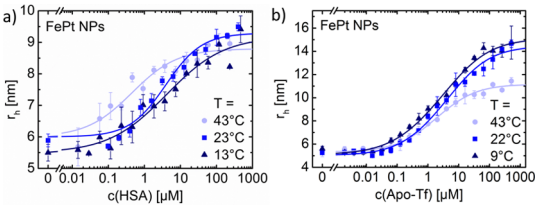

Figure 1. Change of the hydrodynamic radius, r_h, of negatively charged FePt NPs as a function of (a) HSA and (b) apo-Tf concentration in the solution due to protein adsorption at different temperatures *T*.

protein molecules per NP, the resulting shape is aspherical. However, FCS is not sensitive to small deviations from a spherical shape. In fact, in the analysis, we have made the approximation that the shape of the NPs remains spherical upon protein binding.

In accordance with our previous study[21] at room temperature HSA adsorption increases with protein concentration in the solution up to the formation of a protein monolayer, as we have observed *in situ* by using FCS. In Figure 1a, we show HSA monolayer formation for a set of three temperatures (13, 23, 43 °C), as inferred from (i) the observed saturation behavior, *i.e.*, the NP size does not continue to increase beyond a certain HSA concentration, and (ii) the increase in NP size due to HSA binding, which corresponds to the physical size of the HSA molecules. The structure of HSA can be modeled as a 3 nm thick equilateral triangle with sides that are 8 nm long. At 13 and 23 °C the thickness of the protein corona is in agreement with our previous results taken at room temperature, $r_h \approx 3.3$ nm.[21,24] The measured protein corona thickness of 3.3 nm indicates that the HSA molecules adsorb with their triangular surface facing the NPs, supposedly *via* the big, positively charged patch on the surface of one of the two triangular faces, which binds to the negatively charged NPs *via* Coulomb interactions.[24] At 43 °C, the radius increase upon HSA binding is slightly smaller, which may result from an enhanced flexibility of the polymer shell wrapping the FePt core of the NPs at higher temperature, so that the adsorbed HSA proteins may partially penetrate the shell, leading to an overall radius increase just slightly below 3.3 nm. Most remarkable, however, is the finding that the binding affinity displays a marked temperature dependence, as seen from the values of K'_D, the concentration at half coverage (Table 2). Surprisingly, K'_D decreases with temperature, so the highest protein binding affinity is found at the highest temperature. Usually, one would expect that a system tends to dissociate into its individual components at higher temperature so as to increase the overall translational entropy. The observed stronger binding of HSA to the NPs at 43 °C, however, may arise from structural fluctuations of the proteins and/or the polymer shell around the NPs, which will be enhanced at higher temperature. These could induce structural changes that lead to a free energy-optimized binding interface.

We also note that the maximum number, N_{max}, of HSA molecules per NP appears to decrease at 43 °C (Table 2). The N_{max} values, however, should be taken with a grain of salt. They are based on a geometrical model that assumes (1) that the NPs have a smooth spherical surface and (2) that the added volume due to protein adsorption, which we infer from the change in r_h, is homogeneously filled with protein. At 43 °C, N_{max} will be underestimated if HSA molecules partially enter the polymer shell, as we expect from the smaller thickness of the protein corona. At 23 or 13 °C, N_{max} may be overestimated if the monolayer formed is not completely densely packed.

The binding of apo-Tf onto the FePt NPs was studied at 9, 22, and 43 °C (*cf.* Figure 1b). The data indicate formation of a monolayer of apo-Tf around each NP under saturating conditions.[22] As for HSA, the affinity of apo-Tf toward the FePt NPs is greater at 43 °C than at room temperature, as indicated by the smaller ligand concentration producing half occupation K'_D at 43 °C (*cf.* Table 2). The affinities of Apo-Tf toward the NPs are identical within experimental error at 22 °C and at 9 °C. The measured protein corona thickness is also very similar at 22 and 9 °C, *i.e.*, 9.3 and 10 nm. The overall size of apo-Tf protein is around $4.2 \times 10 \times 7$ nm^3. It consists of two identical subunits each having dimensions of $4.2 \times 5 \times 7$ nm^3.[25] Because the thickness of the protein corona correlates with one dimension of the protein, Apo-Tf presumably binds to the NPs with the 4.2×7 nm^2 face. We note that, in earlier experiments,[22] we had observed an apo-Tf corona of 7 nm, which suggests that apo-Tf binds to the NP surface with the 4.2×10 nm^2 face. Considering the surface charge and the structure of apo-Tf (*cf.* the Supporting Information) and assuming that apo-Tf binds to the negatively charged NPs *via* positive patches on its surface, apo-Tf may be able to adsorb to the NPs with the 4.2×7 nm^2 as well as with the 4.2×10 nm^2 face. In fact, we have observed different corona thicknesses on apo-Tf with different protein batches purchased from the same supplier. For the same batch of apo-Tf, however, the results were always reproducible. At 43 °C, the experiments revealed a 3 to 4 nm reduced thickness of the protein corona as compared with 22 or 9 °C. Therefore, the added volume due to apo-Tf adsorption is significantly smaller, which results in only 17 apo-Tf molecules attached per NP under saturation conditions in our analysis (*cf.* Table 2). As for HSA, this may be due to conformational changes of the proteins upon binding, which could involve changes in how the positive patches on the surface of the proteins are exposed to the solvent. Consequently, the overall orientation of the proteins on the surface may also change. Another possible scenario is that the proteins

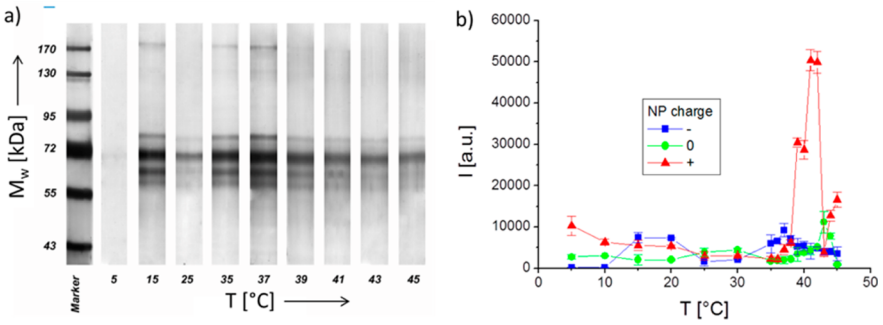

Figure 2. (a) SDS-PAGE gel of proteins adsorbed onto the surfaces of negatively charged FeO_x NPs after 1 h incubation in FBS at different temperatures. The molecular weights M_w of the proteins in the marker lane on the left are reported for reference. (b) Quantification of the amount of adsorbed proteins on negatively charged (−), neutral (0), and positively charged (+) NPs as derived from the total band intensities of proteins on the SDS-PAGE gels.

partially penetrate the polymer shell, which may be more flexible at this temperature.

Compound-Specific Adsorption of FBS onto FeO_x NPs. Because magnetic separation of the small, colloidally stable, and highly defined FePt NPs was not feasible due to their small size, data involving removal of unbound protein were carried out with the bigger FeO_x NPs. Structural and colloidal properties of dextran-coated FeO_x NPs were investigated with TEM and DLS. The diameter d_c of the inorganic FeO_x core and the hydrodynamic diameter d_h (as determined in PBS), respectively, are included in Table 1. Due to their larger size, these NPs allow for convenient magnetic separation and, thus, removal of unbound proteins. However, the NP cores have a relatively large size distribution and were partly agglomerated (especially the positively charged NPs), as indicated by hydrodynamic diameters much bigger than the diameters of the inorganic cores (*cf.* the Supporting Information). After incubation of the NPs in protein solution (10% FBS + 90% PBS) for 1 h at different temperatures, unbound or loosely bound proteins were removed by two washing steps in succession, during which the magnetic NPs were trapped in a strong magnetic field, while the eluted washing solutions were discarded. All washing steps were performed using prewarmed/-cooled washing solutions of the same temperature as during incubation. Only strongly attached proteins are retained on the NP surface after washing.

The proteins were afterward extracted from the NPs and then run on SDS-PAGE. The amount of protein was inferred from the integrated intensities along each line in the gel. An example of a gel with proteins that had adsorbed onto negatively charged NPs (incubated at different temperatures) is shown in Figure 2a (further data and details are included in the Supporting Information). The temperature dependence of the total amount of adsorbed proteins is reported in Figure 2b for the three types of FeO_x NPs. Our data indicate that even a slight temperature increase can already cause remarkable changes in the band intensities and, consequently, the composition of the protein adsorption layer. In order to challenge these findings, control experiments were performed to study the influence of possible sources of error. (i) As FeO_x NPs were found to be partly agglomerated, batch-to-batch variations were probed. (ii) During the washing steps, some NPs might get lost and the amount of the detached proteins might also vary. Thus, variations among different purification runs were probed. (iii) SDS-PAGE and the subsequent quantification of protein may introduce errors: therefore, also these variations were also examined. The observed peak variations were below 10%, which in addition to the smooth connection between the data points indicates that the peaks in the amount of detected corona proteins (Figure 2b) are real. The amount of adsorbed proteins was highest around 40 °C. Also, for neutral and negatively charged NPs, less pronounced maxima exist around 43 and 37 °C, respectively.

The contribution of individual proteins to the corona under conditions of varying NP functionalization and incubation temperature was investigated with liquid chromatography/mass spectrometry (LC-MS/MS) (Figure 3). Significant differences were found between the protein profiles at various temperatures. In particular, we focused on the adsorption of three important serum proteins, for which association to FePt NPs has been previously investigated by using FCS: serum albumin (M_w = 66 kDa),[21,24] serotransferrin (M_w = 76 kDa),[22] and apolipoprotein A-I (M_w = 28 kDa).[24] In addition, we also studied alpha-2-HS-glycoprotein (M_w = 49 kDa). The contributions of serum albumin, serotransferrin, apolipoprotein A-I, and alpha-2-HS-glycoprotein demonstrate a temperature-dependent corona. Noticeably, increased protein adsorption can be seen around 40 °C, in particular for positively charged NPs and for alpha-2-HS-glycoprotein. The significance of this peak, which also appears in the SDS-PAGE data (Figure 2), is further strengthened by the fact that it extends consistently over several data points. However, due to the large error bars (*cf.* the Supporting Information) and also due to limited quality of the FeO_x NPs concerning size distribution

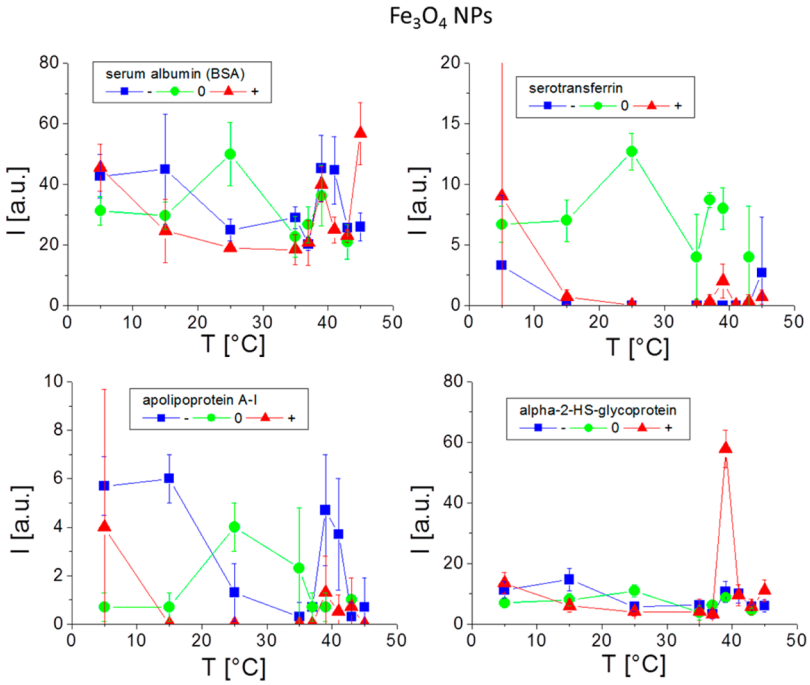

Figure 3. Temperature-dependent amounts of specific proteins in the protein corona of negatively charged (−), positively (+), charged, and neutral (0) FeO_x NPs, as obtained from LC-MS/MS data. Mean values over three independent measurements are shown with their corresponding standard deviations.

and colloidal dispersion, the data presented here rather have to be interpreted in a qualitative than in a quantitative way. Also, in the FCS data on FePt NPs, a noticeable difference in the protein corona was observed between room temperature and 43 °C. Thus, our data indicate that the composition of the corona strongly depends on the temperature at which the corona is formed (*i.e.*, the incubation temperature).

NP Interaction with Cells. Cellular endocytotic processes are intrinsically temperature-dependent.[26−28] For example, below 4 °C, active internalization is suppressed. Also the protein layers formed on the NP surface affect their uptake and trafficking inside cells.[29,30] We have demonstrated above that the formation of the protein corona is temperature-dependent. Thus one may ask how much of this temperature-dependent formation of the protein corona is reflected in temperature-dependent internalization of NPs by cells. In order to investigate this, uptake of fluorescence-labeled FePt NPs under serum-free and serum-containing conditions was analyzed with confocal microscopy at different incubation temperatures. Active cellular uptake of NPs involves the transfer of NPs into endosomes and subsequently lysosomes.[1] Thus we quantified uptake in terms of the amount of NPs found inside cells and of the amount of NPs found inside lysosomes.

In accordance with previous studies,[14,22,30,31] we noticed that NP uptake was reduced by protein corona formation compared to bare NPs, as inferred from measurements with incubation in serum-containing *versus* serum-free medium (*cf.* Figure 4c,f). We also observed a clear enhancement of NP uptake (in terms of mean NP intensity inside cells) with increasing temperatures, as well as with serum-free (Figure 4a) and serum-containing media (*cf.* Figure 4b). This trend was not as clear in the case where only NPs inside lysosomes were considered (*cf.* Figure 4c,d). In order to infer whether the protein corona plays a role in the temperature-dependent uptake of NPs, we analyzed the temperature dependence of the ratio of the uptake of NPs under serum-free and serum-containing conditions. Within our experimental errors we at best can speculate that the amount of NPs internalized by cells may rise faster with temperature under serum-free than under serum-containing conditions (*cf.* Figure 4c). In the case where NP uptake is quantified only by NPs localized inside lysosomes a different tendency was observed (*cf.* Figure 4f). Thus, even without considering that the impact of identical NPs on various cells can be significantly different[4,32,33] our data do not allow for deriving a sharp conclusion about the correlation between the temperature-dependence of protein corona formation and NP uptake. Taking into account the different methods of quantification we applied, neither can we prove that the temperature-dependent formation of the protein corona around NPs may have some influence on the temperature-dependence of NPs uptake by cells, nor can we claim the opposite. Other temperature-dependent effects, such as active NP transport, are likely to play important roles in the temperature dependence in NP uptake, and thus the importance of the temperature dependence of protein

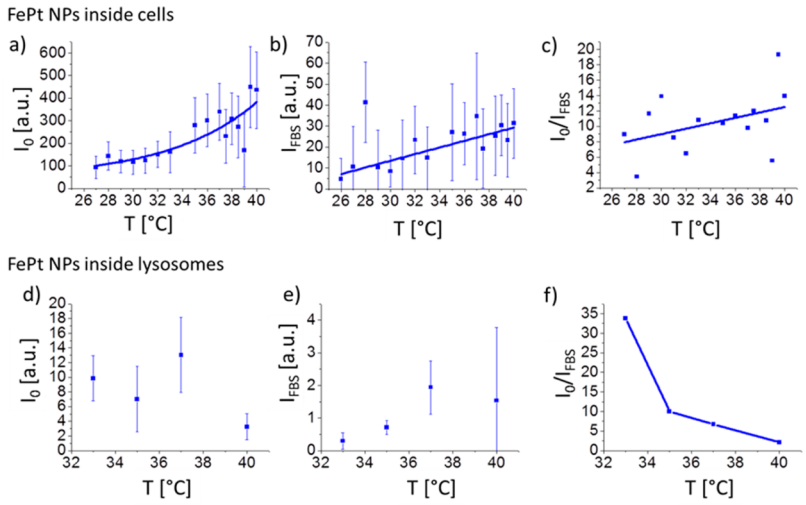

Figure 4. Uptake of fluorescently labeled FePt(−) NPs by HeLa cells after 3 h of incubation. Mean fluorescence intensities *I* of NPs upon using serum-free (I_0) and serum-containing (I_{FBS}) culture media are plotted. (a, b, c) Mean fluorescence intensities *I* of NPs that are localized inside cells. Each data point corresponds to the mean value of at least 2000 analyzed cells and the corresponding standard deviation. Exponential curves are added in order to serve as guide to the eyes. Also the ratio I_0/I_{FBS} is plotted for the different incubation temperatures *T*. (d, e, f) Mean fluorescence intensities *I* of NPs that are localized inside lysosomes. Each data point corresponds to the mean value of at least 30 analyzed cells and the corresponding standard deviation.

corona formation on the temperature dependence in NP uptake can be fully elucidated with more sophisticated assays. Also entanglement of size and protein corona formation needed to be considered, as NP uptake is also size-dependent.[34] In Figure 1 we demonstrated that at the same protein concentration the effective NP radius can be significantly different due to different corona formation, and a detailed analysis also would need to take size effects into account.

CONCLUSIONS

In this study, we have investigated the influence of the exposure temperature, ranging from 5 to 45 °C, on the formation and composition of the protein corona on magnetic NPs. The influence of temperature on NP−cell interactions was also investigated. We have shown that changes in the incubation temperature can cause significant effects in protein corona formation and composition, although this is not necessarily always the case. Temperature effects for the NPs investigated by us were especially pronounced in the physiologically highly relevant temperature window of 37−41 °C. Thus, our findings suggest that studies on the formation of a protein corona on NPs should be carried out at well-controlled temperatures to enable comparison and reproduction of results from different laboratories. The results presented are expected to apply to other classes of NPs, such as fluorescent or plasmonic NPs, with similar surface functionalization, although we did not prove this yet experimentally.

MATERIALS AND METHODS

Synthesis of FePt NPs and Investigation of Adsorbed HSA with FCS. Synthesis of polymer-coated FePt NPs with a fluorophore (DY-636) in the polymer shell has been reported previously.[21] Our two-focus fluorescence correlation spectroscopy setup has recently been described.[24] For incubation with proteins, FePt NPs and proteins were mixed and incubated at a controlled temperature, *T*, for 10 min. HSA and apo-Tf were purchased from Sigma Aldrich as lyophilized powders (A8763 and T4382, respectively). The proteins were suspended in PBS without Ca^{2+} and Mg^{2+} ions (PAA Laboratories) at room temperature at a concentration of 1 mM or less. Subsequently, FCS measurements were carried out for 4 min at the same temperature, *T*. A 40 μL amount of solution was filled into a sample chamber consisting of a small borosilicate glass cylinder glued to a coverslip with epoxy. The sample chamber was kept in a small water bath within an aluminum block heated or cooled to the desired temperature with a Peltier element. Thermal expansion effects due to temperature changes in the objective led to small variations in the focusing properties and, thus, to slight changes of the confocal volume, as was observed by measuring the point spread function (PSF) using laser light reflected off 100 nm gold NPs. We compensated the temperature effect by changing the position of the correction collar normally used to correct for different coverslip thicknesses. The position of the correction collar was adjusted so as to achieve maximum fluorescence intensity, which also correlates with the smallest dimensions of the measured confocal volume. Furthermore, we measured deviations in the interfoci distance resulting from temperature changes with a reference sample, Atto655 in buffer solution. The measured size of the NPs was corrected according to the calibration obtained with the reference sample. Temperature was directly measured in the sample solution. Hydrodynamic radii, r_h, were determined by FCS and plotted *versus* the HSA concentration in solution, *c*(HSA), as shown in Figure 1. At saturation, the hydrodynamic radius of one NP was calculated according to[21]

$$r_h(N_{max}) = r_h(0)\sqrt[3]{1 + cN_{max}} \quad (1)$$

where $c = V_p/V_0$ is the volume ratio of protein molecules to NP. For the NPs, the volume was simply calculated by using $V_0 = (4\pi/3)(r_h(0))^3$. For apo-Tf, the volume was estimated from the physical dimensions, *i.e.*, $V_p = 10 \times 7 \times 4.2 = 294$ nm^3. Likewise,

for HSA, the volume of a triangular prism with 8 nm side length and 3 nm thickness was computed, *i.e.*, $V_p = 3 \times (8/2) \times (8^2 - 4^2)^{1/2} = 83\ nm^3$. Note that, for HSA, which is a compact globular protein, V_p can equally well be calculated by using $V_p = (M_w/N_A)/\rho_p$, with the molecular weight, M_w, of HSA, Avogadro's constant, N_A, and the protein density, $\rho_p = 1.35\ g/cm^3$. N_{max} is the maximum number of adsorbed molecules. Concentration-dependent adsorption was described by the Hill equation,

$$N = N_{max} \frac{1}{1 + (K'_D/[Pr])^n} \quad (2)$$

where N is the number of adsorbed protein molecules per NP, K'_D represents the concentration of protein molecules for half coverage, and n is the Hill coefficient, which determines the steepness of the binding curve.[21]

Synthesis of FeO_x NPs and Investigation of Adsorbed FBS with PAGE and MS. Syntheses of dextran-coated FeO_x NPs (SPIONs, inorganic core diameter) with negative, neutral, and positive surface charges were performed according to our previously published protocols (hydrodynamic radii together with their characterization are presented in the Supporting Information).[35] To study the interactions of the NPs with FBS, 100 μL of NP solution (with a concentration of 100 μg/mL) was mixed with 900 μL of FBS and incubated at T = 5, 15, 25, 35, 37, 39, 41, 43, and 45 °C. The protein/NP mixtures were run through a strong magnetic field using a magnetic-activated cell sorting system. NPs were trapped inside the magnetic column, and the flow-through fraction (two washing steps with 500 μL of PBS buffer) was removed. We ensured that all washing solutions were at the same temperature as the media used during incubation. Finally, the column was removed from the magnetic field, and the released NPs were collected. The protein/NP mixtures were immediately resuspended in protein loading buffer containing 10% dithiothreitol, followed by boiling for 5 min at 100 °C to remove the proteins from the NPs.[3] To quantify the amount of proteins on the surface of the various NPs, equal sample volumes of the solution were loaded into sodium dodecyl sulfate polyacrylamide gel electrophoresis (1D SDS-PAGE). Gel electrophoresis was carried out at 120 V, 400 mA, for about 60 min each, until the proteins approached the end of the gel. While the NPs stick in the wells of the gels, the desorbed proteins migrate in the applied electric field. The gels were stained by silver nitrate in order to visualize the proteins and scanned using a Biorad GS-800 calibrated densitometer scanner, and gel densitometry was performed using Image J (1.410 version). Intensity profiles of the stained proteins along the migration direction of the proteins were recorded to quantify the total amount of protein in each lane and the contribution of the proteins of different molecular weight to the total amount. An example of a gel after SDS-PAGE is shown in Figure 2a. To determine the relative amounts of proteins adsorbed onto different NPs, the collected proteins were digested with trypsin and analyzed by LC-MS/MS. A semiquantitative evaluation of the data was done by using the peptide spectrum matches (*i.e.*, "spectral counts") assigned to a distinct protein by Proteome Discoverer software.

Uptake of FePt NPs by Cells. HeLa cells were incubated with polymer-coated FePt NPs with integrated fluorophore (DY-636) at different temperatures for 3 h with and without serum (FBS) in the culture medium. Nuclei, membranes, and lysosomes of the cells were stained, and fluorescence images of these cellular compartments together with images of the NP distribution were recorded with confocal microscopy (for details refer to the Supporting Information). Cellular compartments were identified with the open source software CellProfiler. NPs located in the specific compartments (here either inside cells or inside lysosomes) were identified by overlay of a mask corresponding to the locations of the compartments with the image of the NP distribution.[36] As well, the total amount of NPs incorporated per cell (as quantified by the mean fluorescence intensity I inside cells), as the amount of NPs that co-localized with the lysosome (as quantified by the mean fluorescence intensity I inside lysosomes),[37] was determined. Please note the limited depth resolution of confocal microscopy, which makes it complicated to distinguish between NPs only adherent to the outer cell surface and internalized NPs. One could clearly distinguish between both cases using pH-sensitive fluorophores attached to the NPs[38,39] In our case we also stained the cell membrane. We did not observe a significant amount of NPs at positions close to the cell membrane, and thus the error in the quantification of internalized NPs by wrongfully counting also NPs attached to the outer membrane is very small.

Conflict of Interest: The authors declare no competing financial interest.

Acknowledgment. This work was supported by the Deutsche Forschungsgemeinschaft DFG (grants CFN, NI291/7, and NI291/8 to G.U.N. and grant PA794/4-2 to W.J.P.). The authors thank Faheem Amin for helping with the synthesis and polymer coating of FePt NPs, Dr. Andreas Schaper for discussions about TEM, Alexander Hepting for his efforts with the temperature-controlled measurement chamber, and Dominik Hühn for proofreading the manuscript.

Supporting Information Available: Full methodology and additional data are available free of charge *via* the Internet at http://pubs.acs.org.

REFERENCES AND NOTES

1. Nel, A. E.; Madler, L.; Velegol, D.; Xia, T.; Hoek, E. M. V.; Somasundaran, P.; Klaessig, F.; Castranova, V.; Thompson, M. Understanding Biophysicochemical Interactions at the Nano-Bio Interface. *Nat. Mater.* **2009**, *8*, 543–557.
2. Mahmoudi, M.; Lynch, I.; Ejtehadi, M. R.; Monopoli, M. P.; Bombelli, F. B.; Laurent, S. Protein-Nanoparticle Interactions: Opportunities and Challenges. *Chem. Rev.* **2011**, *111*, 5610–5637.
3. Monopoli, M. P.; Walczyk, D.; Campbell, A.; Elia, G.; Lynch, I.; Bombelli, F. B.; Dawson, K. A. Physical-Chemical Aspects of Protein Corona: Relevance to *in Vitro* and *in Vivo* Biological Impacts of Nanoparticles. *J. Am. Chem. Soc.* **2011**, *133*, 2525–2534.
4. Laurent, S.; Burtea, C.; Thirifays, C.; Hafeli, U. O.; Mahmoudi, M. Crucial Ignored Parameters on Nanotoxicology: The Importance of Toxicity Assay Modifications and "Cell Vision". *PLoS One* **2012**, *7*, e29997.
5. Walczyk, D.; Bombelli, F. B.; Monopoli, M. P.; Lynch, I.; Dawson, K. A. What the Cell "Sees" in Bionanoscience. *J. Am. Chem. Soc.* **2010**, *132*, 5761–5768.
6. Cedervall, T.; Lynch, I.; Foy, M.; Berggad, T.; Donnelly, S.; Cagney, G.; Linse, S.; Dawson, K. Detailed Identification of Plasma Proteins Adsorbed on Copolymer Nanoparticles. *Angew. Chem., Int. Ed.* **2007**, *46*, 5754–5756.
7. Lundqvist, M.; Stigler, J.; Cedervall, T.; Berggard, T.; Flanagan, M. B.; Lynch, I.; Elia, G.; Dawson, K. The Evolution of the Protein Corona around Nanoparticles: A Test Study. *ACS Nano* **2011**, *5*, 7503–7509.
8. Tenzer, S.; Docter, D.; Rosfa, S.; Wlodarski, A.; Kuharev, J.; Rekik, A.; Knauer, S. K.; Bantz, C.; Nawroth, T.; Bier, C.; *et al.* Nanoparticle Size Is a Critical Physicochemical Determinant of the Human Blood Plasma Corona: A Comprehensive Quantitative Proteomic Analysis. *ACS Nano* **2011**, *5*, 7155–7167.
9. Maiorano, G.; Sabella, S.; Sorce, B.; Brunetti, V.; Malvindi, M. A.; Cingolani, R.; Pompa, P. P. Effects of Cell Culture Media on the Dynamic Formation of Protein-Nanoparticle Complexes and Influence on the Cellular Response. *ACS Nano* **2010**, *4*, 7481–7491.
10. Gebauer, J. S.; Malissek, M.; Simon, S.; Knauer, S. K.; Maskos, M.; Stauber, R. H.; Peukert, W.; Treuel, L. Impact of the Nanoparticle-Protein Corona on Colloidal Stability and Protein Structure. *Langmuir* **2012**, *28*, 9673–9679.
11. Casals, E.; Pfaller, T.; Duschl, A.; Oostingh, G. J.; Puntes, V. F. Time Evolution of the Nanoparticle Protein Corona. *ACS Nano* **2010**, *4*, 3623–3632.
12. Milani, S.; Bombelli, F. B.; Pitek, A. S.; Dawson, K. A.; Radler, J. Reversible *versus* Irreversible Binding of Transferrin to Polystyrene Nanoparticles: Soft and Hard Corona. *ACS Nano* **2012**, *6*, 2532–2541.

13. Walkey, C. D.; Chan, W. C. Understanding and Controlling the Interaction of Nanomaterials with Proteins in a Physiological Environment. *Chem. Soc. Rev.* **2012**, *41*, 2780–2799.
14. Hühn, D.; Kantner, K.; Geidel, C.; Brandholt, S.; De Cock, I.; Soenen, S. J. H.; Rivera Gil, P.; Montenegro, J.-M.; Braeckmans, K.; Müllen, K.; *et al*. Polymer-Coated Nanoparticles Interacting with Proteins and Cells: Focusing on the Sign of the Net Charge. *ACS Nano* **2013**, *7*, 3253–3263.
15. Lesniak, A.; Campbell, A.; Monopoli, M. P.; Lynch, I.; Salvati, A.; Dawson, K. A. Serum Heat Inactivation Affects Protein Corona Composition and Nanoparticle Uptake. *Biomaterials* **2010**, *31*, 9511–9518.
16. Petersdorf, R. G. Chills and Fever. In *Harrison's Principles of Internal Medicine*; McGraw-Hill: New York, 1974.
17. Hasday, J. D.; Singh, I. S. Fever and the Heat Shock Response: Distinct, Partially Overlapping Processes. *Cell Stress Chaperones* **2000**, *5*, 471–480.
18. Rhoades, R. A.; Pflanzer, R. G. *Human Physiology*.; Saunders College Publishing: Philadelphia, PA, 1989; pp 823−840.
19. Yang, J. M.; Yang, H.; Lin, L. W. Quantum Dot Nano Thermometers Reveal Heterogeneous Local Thermogenesis in Living Cells. *ACS Nano* **2011**, *5*, 5067–5071.
20. Donner, J. S.; Thompson, S. A.; Kreuzer, M. P.; Baffou, G.; Quidant, R. Mapping Intracellular Temperature Using Green Fluorescent Protein. *Nano Lett.* **2012**, *12*, 2107–2111.
21. Röcker, C.; Pötzl, M.; Zhang, F.; Parak, W. J.; Nienhaus, G. U. A Quantitative Fluorescence Study of Protein Monolayer Formation on Colloidal Nanoparticles. *Nat. Nanotechnol.* **2009**, *4*, 577–580.
22. Jiang, X.; Weise, S.; Hafner, M.; Röcker, C.; Zhang, F.; Parak, W. J.; Nienhaus, G. U. Quantitative Analysis of the Protein Corona on FePt Nanoparticles Formed by Transferrin Binding. *J. R. Soc., Interface* **2010**, *7*, S5–S13.
23. Lehmann, A. D.; Parak, W. J.; Zhang, F.; Ali, Z.; Röcker, C.; Nienhaus, G. U.; Gehr, P.; Rothen-Rutishauser, B. Fluorescent-Magnetic Hybrid Nanoparticles Induce a Dose-Dependent Increase in Proinflammatory Response in Lung Cells *in Vitro* Correlated with Intracellular Localization. *Small* **2010**, *6*, 753–762.
24. Maffre, P.; Nienhaus, K.; Amin, F.; Parak, W. J.; Nienhaus, G. U. Characterization of Protein Adsorption onto FePt Nanoparticles Using Dual-Focus Fluorescence Correlation Spectroscopy. *Beilstein J. Nanotechnol.* **2011**, *2*, 374–383.
25. Bailey, S.; Evans, R. W.; Garratt, R. C.; Gorinsky, B.; Hasnain, S.; Horsburgh, C.; Jhoti, H.; Lindley, P. F.; Mydin, A.; Sarra, R.; *et al*. Molecular-Structure of Serum Transferrin at 3.3-A Resolution. *Biochemistry* **1988**, *27*, 5804–5812.
26. Mamdouh, Z.; Giocondi, M. C.; Laprade, R.; LeGrimellec, C. Temperature Dependence of Endocytosis in Renal Epithelial Cells in Culture. *Biochim. Biophys. Acta* **1996**, *1282*, 171–173.
27. Weigel, P. H.; Oka, J. A. Temperature-Dependence of Endocytosis Mediated by the Asialoglycoprotein Receptor in Isolated Rat Hepatocytes - Evidence for 2 Potentially Rate-Limiting Steps. *J. Biol. Chem.* **1981**, *256*, 2615–2617.
28. Hong, G. S.; Wu, J. Z.; Robinson, J. T.; Wang, H. L.; Zhang, B.; Dai, H. J. Three-Dimensional Imaging of Single Nanotube Molecule Endocytosis on Plasmonic Substrates. *Nat. Commun.* **2012**, 3.
29. Jedlovszky-Hajdu, A.; Bombelli, F. B.; Monopoli, M. P.; Tombacz, E.; Dawson, K. A. Surface Coatings Shape the Protein Corona of Spions with Relevance to Their Application *in Vivo*. *Langmuir* **2012**, *28*, 14983–14991.
30. Lesniak, A.; Fenaroli, F.; Monopoli, M. R.; Aberg, C.; Dawson, K. A.; Salvati, A. Effects of the Presence or Absence of a Protein Corona on Silica Nanoparticle Uptake and Impact on Cells. *ACS Nano* **2012**, *6*, 5845–5857.
31. Mirshafiee, V.; Mahmoudi, M.; Lou, K.; Cheng, J.; Kraft, M. L. Protein Corona Significantly Reduces Active Targeting Yield. *Chem. Commun.* **2013**, *49*, 2557–2559.
32. Mahmoudi, M.; Laurent, S.; Shokrgozar, M. A.; Hosseinkhani, M. Toxicity Evaluations of Superparamagnetic Iron Oxide Nanoparticles: Cell "Vision" *versus* Physicochemical Properties of Nanoparticles. *ACS Nano* **2011**, *5*, 7263–7276.
33. Mahmoudi, M.; Saeedi-Eslami, S. N.; Shokrgozar, M. A.; Azadmanesh, K.; Hassanlou, M.; Kalhor, H. R.; Burtea, C.; Rothen-Rutishauser, B.; Laurent, S.; Sheibani, S.; *et al*. Cell "Vision": Complementary Factor of Protein Corona in Nanotoxicology. *Nanoscale* **2012**, *4*, 5461–5468.
34. Chithrani, B. D.; Chan, W. C. W. Elucidating the Mechanism of Cellular Uptake and Removal of Protein-Coated Gold Nanoparticles of Different Sizes and Shapes. *Nano Lett.* **2007**, *7*, 1542–1550.
35. Mahmoudi, M.; Simchi, A.; Milani, A.; Stroeve, P. Cell Toxicity of Superparamagnetic Iron Oxide Nanoparticles. *J. Colloid Interface Sci.* **2009**, *336*, 510–518.
36. Rivera Gil, P.; Yang, F.; Thomas, H.; Li, L.; Terfort, A.; Parak, W. J. Development of an Assay Based on Cell Counting with Quantum Dot Labels for Comparing Cell Adhesion within Cocultures. *Nano Today* **2011**, *6*, 20–27.
37. Schweiger, C.; Hartmann, R.; Zhang, F.; Parak, W. J.; Kissel, T.; Rivera Gil, P. Quantification of the Internalization Patterns of Superparamagnetic Iron Oxide Nanoparticles with Opposite Charge. *J. Nanobiotechnol.* **2012**, *10*, 28.
38. Semmling, M.; Kreft, O.; Muñoz Javier, A.; Sukhorukov, G. B.; Käs, J.; Parak, W. J. A Novel Flow-Cytometry-Based Assay for Cellular Uptake Studies of Polyelectrolyte Microcapsules. *Small* **2008**, *4*, 1763–1768.
39. Zhang, F.; Lees, E.; Amin, F.; Rivera Gil, P.; Yang, F.; Mulvaney, P.; Parak, W. J. Polymer-Coated Nanoparticles: A Universal Tool for Biolabelling Experiments. *Small* **2011**, *7*, 3113–3127.